Arrestin Isoforms Dictate Differential Kinetics of A_{2B} Adenosine Receptor Trafficking†

Stuart J. Mundell,‡ Anne-Lise Matharu,§ Eamonn Kelly,§ and Jeffrey L. Benovic*,‡

Department of Microbiology and Immunology, Kimmel Cancer Center, Thomas Jefferson University, Philadelphia, Pennsylvania 19107 and Department of Pharmacology, School of Medical Sciences, University Walk, Bristol, BS8 1TD, UK

Received May 12, 2000; Revised Manuscript Received August 14, 2000

ABSTRACT: Adenosine mediates the activation of adenylyl cyclase via its interaction with specific A_{2A} and A_{2B} adenosine receptors. Previously, we demonstrated that arrestins are involved in rapid agonist-promoted desensitization of the A_{2B} adenosine receptor (A_{2B}AR) in HEK293 cells. In the present study, we investigate the role of arrestins in A_{2B}AR trafficking. Initial studies demonstrated that HEK293 cells stably expressing arrestin antisense constructs, which reduce endogenous arrestin levels, effectively reduced A_{2B}AR internalization. A_{2B}AR recycling after agonist-induced endocytosis was also significantly impaired in cells with reduced arrestin levels. Interestingly, while overexpression of arrestin-2 or arrestin-3 rescued A_{2B}AR internalization and recycling, arrestin-3 promoted a significantly faster rate of recycling as compared to arrestin-2. The specificity of arrestin interaction with A_{2B}ARs was further investigated using arrestins fused to the green fluorescent protein (arr-2-GFP and arr-3-GFP). Both arrestins underwent rapid translocation (<1 min) from the cytosol to the plasma membrane following A_{2B}AR activation. However, longer incubations with agonist (>10 min) revealed that arr-2-GFP but not arr-3-GFP colocalized with the A_{2B}AR in rab-5 and transferrin receptor containing early endosomes. At later times, the A_{2B}AR but not arr-2-GFP was observed in an apparent endocytic recycling compartment. Thus, while arrestin-2 and arrestin-3 mediate agonist-induced A_{2B}AR internalization with relative equal potency, arrestin isoform binding dictates the differential kinetics of A_{2B}AR recycling and resensitization.

Adenosine modulates the physiological function of many cell types through its interaction with at least four distinct G protein-coupled receptors (GPCRs)[1] termed A_1, A_{2A}, A_{2B}, and A_3 adenosine receptors (ARs) (*1*). Both A_2AR subtypes are known to couple in a stimulatory fashion to adenylyl cyclase (*1*, *2*), although the A_{2B}AR can also couple to $G_{q/11}$ to stimulate inositol trisphosphate and calcium accumulation (*3*). Although our knowledge of A_{2B}AR function and regulation has lagged behind that of the other subtypes, recent studies implicating A_{2B}AR in the regulation of gene expression, cell growth, vascular tone, and neurosecretion underscore the importance of this receptor in cellular physiology (*2*).

Both A_2ARs undergo rapid agonist-induced desensitization (*4*). Previous studies have implicated receptor phosphorylation by G protein-coupled receptor kinase-2 (GRK2) as the likely mechanism by which A_2ARs undergo rapid desensitization (*5*, *6*). Agonist-dependent phosphorylation of GPCRs by GRKs promotes the high affinity binding of arrestins (*7*), which in turn sterically inhibit G protein interaction thereby terminating agonist-mediated signaling (*8*, *9*). Recent studies have shown that the nonvisual arrestins, arrestin-2 and arrestin-3, also facilitate internalization of GPCRs (*10*−*12*). Arrestin binding directs GPCRs to a clathrin-mediated endocytic pathway where receptors are internalized and subsequently recycled back to the plasma membrane (*13*, *14*). Mechanistic insight into this process has revealed that nonvisual arrestins can bind to components of clathrin-coated pits such as clathrin and AP2 thereby functioning as adaptor proteins to mediate GPCR uptake into clathrin-coated pits (*11*, *15*, *16*).

Internalization may play divergent roles for different GPCRs. For example, while internalization plays a key role in the resensitization of the β_2-adrenergic receptor (*17*−*19*), it appears to prolong desensitization of the M_4 muscarinic acetylcholine receptor (*20*). Inhibition of internalization has also been shown to differentially affect the desensitization and resensitization of A_{2A} adenosine and secretin receptors while having no effect on IP-prostanoid responses (*21*).

In a recent study, we demonstrated that an antisense strategy could be successfully employed to reduce endogenous arrestin levels and effect changes in the internalization, desensitization, and resensitization of the β_2-adrenergic receptor in HEK293 cells (*22*). In the same study, pretreat-

† This work was supported by NIH Grant GM47417 and by the British Heart Foundation.

* To whom correspondence should be addressed: Jeffrey L. Benovic, Thomas Jefferson University, 233 S. 10th Street, Philadelphia, PA 19107. Telephone: 215-503-4607; fax: 215-923-1098; e-mail: benovic@lac.jci.tju.edu.

‡ Thomas Jefferson University.

§ University Walk, Bristol.

[1] Abbreviations: A_{2B}AR, A_{2B} adenosine receptor; BSA, bovine serum albumin; arr-2-GFP, arrestin-2 green fluorescent protein; arr-3-GFP, arrestin-3 green fluorescent protein; GPCR, G protein-coupled receptor; GRK, G protein-coupled receptor kinase; HA-A_{2B}AR, haemagglutanin-tagged-A_{2B} adenosine receptor; HEK293 cells, human embryonic kidney cells; PBS, phosphate buffered saline.

10.1021/bi0010928 CCC: $19.00
Published on Web 09/28/2000

ment with the adenosine receptor agonist NECA resulted in significantly attenuated desensitization of endogenously expressed A_{2B}AR in the arrestin antisense treated cells. Thus, endogenous arrestins appear to play an important role in regulating the rapid agonist-promoted desensitization of the A_{2B}AR in HEK293 cells.

The mechanisms involved in regulating A_{2B}AR internalization and recycling have yet to be defined. In the present study, we utilized HEK293 cells expressing arrestin-2 and arrestin-3 antisense constructs to investigate the role of arrestins in trafficking of the A_{2B}AR. Arrestin/GPCR specificity was further characterized by examining changes in GFP tagged arrestin-2 and arrestin-3 redistribution induced by A_{2B}-AR activation.

EXPERIMENTAL PROCEDURES

Materials. Human embryonic kidney cells transformed with the EBNA vector (HEK293-EBNA) were purchased from Invitrogen. Dulbecco's modified Eagle's medium (DMEM) and fetal bovine serum were obtained from Life Technologies Inc. Fugene-6 transfection agent, hygromycin, Geneticin, and Expand High Fidelity DNA polymerase were from Roche. Rneasy RNA isolation kit was from Qiagen, murine Moloney leukemia virus reverse transcriptase was from Promega, and pcDNA3 was from Invitrogen. Rhodamine-conjugated-transferrin was purchased from Molecular Probes. All other reagents were from Sigma.

Production of Epitope-Tagged Rat A_{2B}AR. Total RNA was isolated from 30 mg of rat brain using the Rneasy kit according to the manufacturer's instructions. First-strand cDNA was synthesized using 1 μg of RNA primed with oligo dT and murine Moloney leukemia virus reverse transcriptase. The first-strand cDNA was used as template for PCR with Expand High Fidelity DNA polymerase, using primers that include an *Xba*I restriction site at the 5′ end: sense: 5′GACTCTAGAATGCAGCTAGAGACGCAGG3′ and antisense: 5′GACTCTAGATCACAAGCTCAGACTGAAAGT3′. The 1-kb DNA product obtained by PCR was cleaved with *Xba*I and subcloned into pcDNA3 modified to contain a hemagglutinin (HA) epitope-tag at the 5′ end. The sequence of the cDNA was verified by automated DNA sequencing.

Cell Culture and Transfection. HEK293 cells were maintained in DMEM supplemented with 10% fetal bovine serum, 100 units/mL penicillin G, and 100 μg/mL streptomycin sulfate (complete media) at 37 °C in a humidified atmosphere of 95% air, 5% CO_2. For culture of HEK293-EBNA cells stably transfected with pREP4 or pREP4 containing antisense cDNAs for arrestin-2 or arrestin-3, the media was supplemented with 200 μg/mL Geneticin to maintain EBNA expression and 400 μg/mL hygromycin to maintain pREP4 expression (*22*). For transient transfections of pcDNA3-arr-2-GFP or pcDNA3-arr-3-GFP, HEK293 cells were grown in 100-mm dishes to 80−90% confluence and transfected with 0.25−2 μg of DNA using Fugene-6 following the manufacturer's instructions. Cells were incubated with a DNA/Fugene mixture for 24 h, the media was replaced, and the cells were analyzed 48 h after transfection.

Internalization of HA-A_{2B}AR in HEK293 Cells. Internalization of the HA tagged A_{2B}AR (HA-A_{2B}AR) was measured by ELISA as described by Daunt et al. (*23*). Briefly, cells plated at a density of 6×10^5 cells per 60-mm dish were transfected with 5 μg of pcDNA3-HA-A_{2B}AR and then split after 24 h into 24-well tissue culture dishes coated with 0.1 mg/mL poly-L-lysine. Twenty-four hours later, cells were incubated with DMEM containing the nonselective adenosine receptor agonist NECA (0.1 μM−1 mM) for 0−45 min at 37 °C. In experiments examining A_{2B}AR recycling following agonist-induced internalization, cells were subsequently washed three times in warmed DMEM and then incubated with DMEM containing the adenosine receptor antagonist XAC (10 μM) for 30−90 min at 37 °C. Reactions were stopped by removing the media and fixing the cells with 3.7% formaldehyde in TBSC (20 mM Tris, pH 7.5, 150 mM NaCl, and 20 mM $CaCl_2$) for 5 min at room temperature. Cells were washed three times with TBSC, incubated for 45 min with TBSC containing 1% BSA, and then incubated with a primary antibody (anti-HA monoclonal, 1:1000 dilution in TBSC/BSA) for 1 h at room temperature. Cells were washed three times with TBSC, reblocked with TBSC/BSA for 15 min at room temperature, and incubated with secondary antibody (goat anti-mouse conjugated with alkaline phosphatase; 1:1000 dilution in TBSC/BSA) for 1 h at room temperature. Cells were washed three times with TBSC and a colorimetric alkaline phosphatase substrate added. When adequate color change was achieved, 100 μL of sample were added to 100 μL of 0.4 M NaOH to terminate the reaction, and the samples were read at 405 nm using a microplate reader.

Fluorescence Microscopy and Single Cell Imaging. To assess the distribution of arr-2-GFP, arr3-GFP, and HA-A_{2B}-AR receptor in living cells, HEK293 cells (60-mm dish) were transfected with 0.25 μg of arr-2-GFP or arr-3-GFP ± 5 μg of HA-A_{2B}AR. Cells were grown on poly-L-lysine-coated coverslips and mounted on an imaging chamber (Warner Instrument Corp) equipped with an inlet port through which media and drugs could be perfused. To assess HA-A_{2B}AR distribution, cells were incubated for 30 min at 4 °C with rhodamine-conjugated HA antibody. For experiments analyzing transferrin distribution, cells were incubated for 15 min with 200 μg/mL rhodamine-conjugated transferrin on glass coverslips. Cells were washed 3 times with PBS prior to imaging on a Nikon Eclipse E800 fluorescence microscope using a Plan-Apo 60 × 1.40 NA oil immersion objective. Images were collected using QED Camera software and processed with Adobe Photoshop.

For experiments analyzing rab-5 distribution, HA-A_{2B}AR or arr-2-GFP transfected cells were incubated with a rab-5 specific antibody (Santa Cruz Laboratories) for 1 h at 4 °C in DMEM supplemented with 1% BSA. Cells were washed twice with PBS and then treated with drug for 60 min at 37 °C in DMEM. The cells were fixed with 3.7% formaldehyde/PBS for 15 min at room temperature, washed with PBS, and permeabilized with 0.05% Triton X-100/PBS/$CaCl_2$ for 10 min at room temperature. Nonspecific binding was blocked with 0.05% Triton X-100/PBS/$CaCl_2$ containing 5% nonfat dry milk for 30 min at 37 °C. Goat anti-mouse fluorescein-conjugated or goat anti-mouse rhodamine-conjugated secondary antibody (Molecular Probes) was then added at a dilution of 1:150 in 0.05% Triton X-100/PBS/$CaCl_2$ containing 5% nonfat dry milk for 1 h at 37 °C for HA-A_{2B}AR or arr-2-GFP colocalization experiments, respectively. The cells were washed six times with permeabilization buffer with the last wash left at 37 °C for 30 min, and the cells were then

fixed with 3.7% formaldehyde. Coverslips were mounted using Slow-Fade mounting medium (Molecular Probes) and examined by microscopy as described above. For confocal microscopy, cells were prepared in the same manner, and images were obtained on a Bio-Rad MRC-Zeiss Axiovert 100 confocal microscope using a Zeiss Plan-Apo 63 × 1.40 NA oil immersion objective.

Experimental Design and Statistics. Dose response curves were analyzed by the iterative fitting program GraphPAD Prism (GraphPAD Software). Log concentration−effect curves were fitted to logistic expressions for single-site analysis. $t_{0.5}$ values for agonist-induced internalization were obtained by fitting data to a single-exponential curve. Rates of receptor recycling were obtained by fitting data to a linear regression. Where appropriate, statistical significance was assessed by Student's t-test or by two-way ANOVA using GraphPAD Prism.

RESULTS

Three previously characterized HEK293 cell lines with demonstrated reductions in endogenous arrestin-2 and/or arrestin-3 were used in the present study (*22*). The line AS 37, stably transfected with an arrestin-2 antisense construct, exhibits an ~50% reduction in arrestin-2 levels. Lines AS 83, transfected with an arrestin-3 antisense construct and AS 108, transfected with both arrestin antisense constructs, exhibit an ~50% decrease in arrestin-2 and ~75% decrease in arrestin-3 levels. Endogenous arrestin levels in vector-transfected cells were comparable to those in wild-type HEK293 cells.

Pretreatment of wild type or vector transfected HEK293 cells with the adenosine receptor agonist NECA resulted in the rapid desensitization of endogenously expressed A_{2B}AR-coupled adenylyl cyclase activity which reached ~75% of that in nonpretreated cells after 30 min, an effect that was significantly attenuated in the AS 37 and AS 108 lines (*22*). Thus, endogenous arrestins appear to play an important role in regulating the rapid agonist-promoted desensitization of A_{2B}AR in HEK293 cells. We next sought to address the potential role of arrestins in the trafficking of this receptor. The current lack of a selective radioligand for A_{2B}AR precluded analysis of endogenous A_{2B}AR trafficking. Thus, as an alternative approach, we transiently expressed an HA-tagged-A_{2B}AR in arrestin antisense and vector transfected control (Wt) cell lines and subsequently analyzed the agonist- and time-dependent internalization of this receptor by ELISA. In vector-transfected control cells (Wt), a concentration-dependent loss of cell surface HA-A_{2B}AR was observed following a 30-min incubation with NECA (Figure 1, panel A). Conversely, agonist-induced internalization of the HA-A_{2B}AR in arrestin antisense cell lines was markedly attenuated. We next investigated the time course of receptor internalization. In vector-transfected cells, the HA-A_{2B}AR underwent rapid-agonist induced internalization with a $t_{0.5}$ of ~3.6 ± 0.7 min (data not shown). In contrast, arrestin antisense cell lines demonstrated minimal receptor internalization throughout a 45-min exposure to 100 μM NECA.

Since inhibition of β_2-adrenergic (*17*−*19*) and A_{2A} adenosine (*21*) receptor internalization inhibits resensitization, we tested whether A_{2B}AR internalization plays a role in resensitization. Control and antisense cells were treated with 100 μM NECA for 30 min followed by a 60-min washout

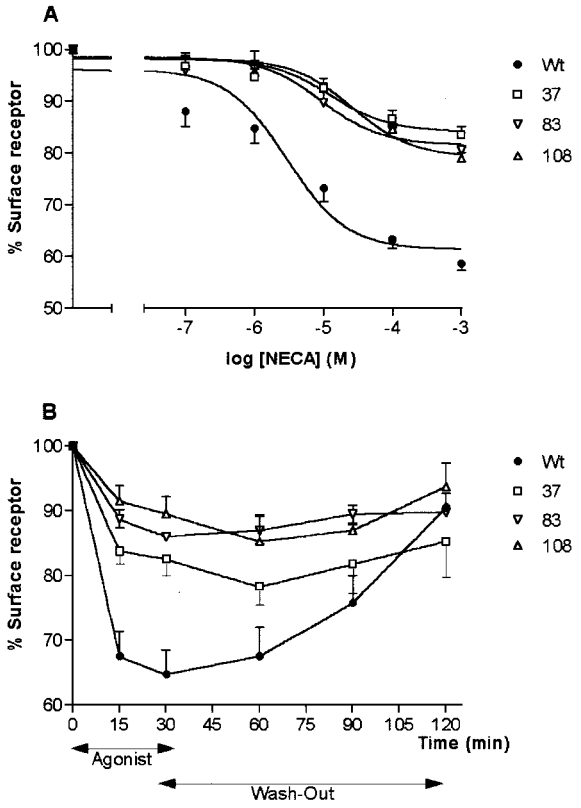

FIGURE 1: Effect of reduced arrestin levels on agonist-induced internalization and recycling of HA-A_{2B}AR. Vector transfected (Wt), AS 37, AS 83, and AS 108 cell lines were transiently transfected with 5 μg of pcDNA3-HA-A_{2B}AR and split into 24-well plates ~24 h after transfection. (A) Cells were incubated with 0.1 μM−1 mM NECA for 20 min and then analyzed for cell surface HA-A_{2B}AR receptors by ELISA as described in Experimental Procedures. (B) Cells were incubated with 100 μM NECA for 30 min at 37 °C, washed three times, and then reincubated with fresh prewarmed medium containing the antagonist XAC for up to 90 min. Cells were washed at the time points shown and analyzed for cell surface HA-A_{2B}AR receptors by ELISA. The data represent means ± SE of five independent experiments.

period to allow the receptor to resensitize. Resensitization of NECA-stimulated adenylyl cyclase activity was almost complete in Wt cells (89.1 ± 8.7%) but was significantly impaired in the arrestin antisense cells (6.5 ± 2.4% and 15.5 ± 5.7% in AS 37 and AS 108 cells, respectively). This suggests that internalization plays a critical role in A_{2B}AR resensitization. We next studied trafficking of the HA-A_{2B}-AR back to the cell surface (recycling) following agonist-induced internalization. Vector transfected, AS 37 and AS 108 cell lines were treated with NECA (100 μM) for 30 min, washed three times, and then allowed to resensitize in fresh medium containing the adenosine receptor antagonist XAC (10 μM). As depicted in Figure 1, panel B, HA-A_{2B}AR recycling following receptor internalization was greatly impaired in cells with reduced arrestin levels as compared to that exhibited in vector transfected controls.

To further examine the role of arrestins in trafficking, we attempted to rescue HA-A_{2B}AR internalization and subsequent recycling by overexpression of either arrestin-2 or arrestin-3 in antisense cells. In these studies, we compared vector transfected control cells (Wt) with AS 108 cells, which display the greatest decrease in both arrestin-2 and arrestin-3 levels. Heterologous expression of either arrestin-2 or arrestin-3 (~10-fold over basal, data not shown) led to a

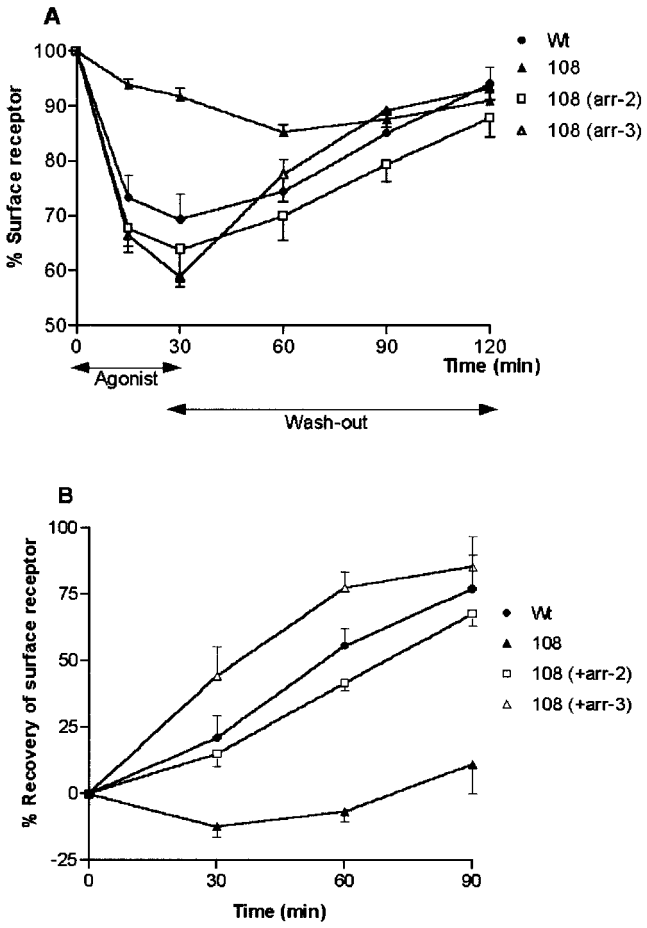

FIGURE 2: Rescue of HA-A_{2B}AR recycling in AS108 cells by overexpression of arrestin-2 or arrestin-3. AS 108 cells were transiently transfected with 5 μg of pcDNA3-HA-A_{2B}AR ± pcDNA3-arrestin-2 (5 μg) or pcDNA3-arrestin-3 (5 μg) and split into 24-well plates ~24 h after transfection. Cells were pretreated with 100 μM NECA for 30 min at 37 °C, washed three times, and then reincubated with fresh prewarmed medium containing the adenosine receptor antagonist XAC for up to 90 min. Cells were washed at the time points shown and then analyzed for cell surface receptors by ELISA as described in Experimental Procedures. The data represent means ± SE of five independent experiments. (A) Represents the percent change in total surface receptor expression. (B) Represents the return of surface receptor to the cell surface following agonist-induced receptor internalization.

full recovery of agonist-promoted receptor internalization in AS 108 cells (Figure 2, panel A) (note that overexpression of a particular arrestin did not affect the endogenous level of the other arrestin isoform, data not shown). The rate and extent of HA-A_{2B}AR internalization were similar in AS 108 cells expressing either arrestin-2 or arrestin-3. Interestingly, receptor recycling was significantly enhanced in AS 108 cells overexpressing arrestin-3 as compared to cells overexpressing arrestin-2 (Figure 2, panels A and B). Although overexpression of either arrestin-2 or arrestin-3 restored effective recycling of the HA-A_{2B}AR, arrestin-3 significantly increased the rate of this process (arr-3, 1.33 ± 0.10%/min; arr-2, 0.65 ± 0.05%/min; Wt, 0.88 ± 0.09%/min over the first 60 min; arr-3 significantly different than arr-2 or Wt, $p > 0.05$ two-way ANOVA) (Figure 2, panel B).

To further examine receptor trafficking, we studied the distribution of the HA-A_{2B}AR in AS 108 cells overexpressing GFP tagged arrestin-2 or arrestin-3 (both ~10-fold over basal, data not shown). As shown in Figure 3, the HA-A_{2B}-

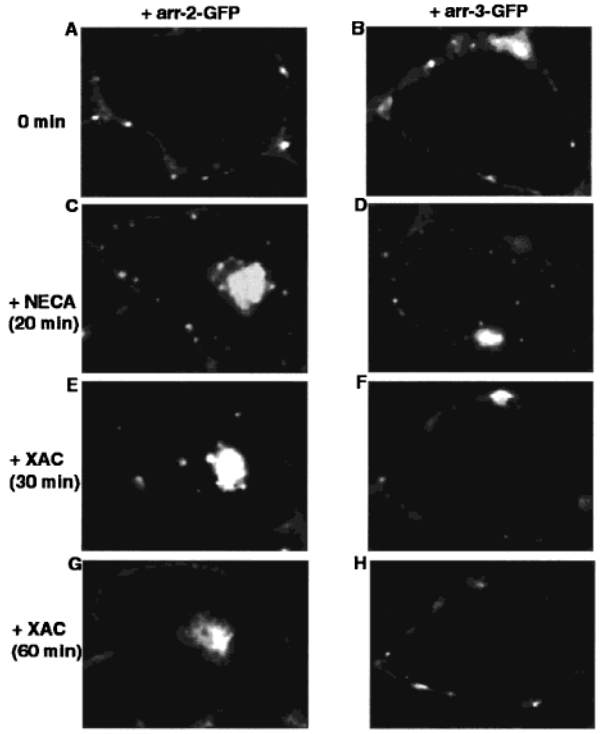

FIGURE 3: Agonist-induced redistribution of HA-A_{2B}AR. AS 108 cells were transfected with 5 μg of HA-A_{2B}AR and 1 μg of arr-2-GFP or arr-3-GFP and then split onto poly-L-lysine-coated glass coverslips. HA-A_{2B}AR was visualized using a rhodamine-conjugated HA antibody. Prior to stimulation and viewing, coverslips were mounted in a chamber at 37 °C as described in Experimental Procedures. The initial membrane localization of receptor is shown in arr-2-GFP (A**)** and arr-3-GFP (B**)** positive cells. The A_2AR agonist NECA (100 μM) (C and D) was added and redistribution of receptor was monitored in real time. Cells were then washed five times with warmed DMEM containing the antagonist XAC (100 μM), and the redistribution of receptor was again monitored in real time as described in Experimental Procedures. Images shown were obtained 20 min (C and D) after agonist addition and then 30 (E and F) and 60 min (G and H) after agonist washout.

AR (as visualized with a rhodamine-conjugated HA-primary antibody) was localized at the cell surface prior to agonist stimulation (Figure 3, panels A and B). Following NECA stimulation (20 min; 100 μM), HA-A_{2B}ARs underwent redistribution into a distinct punctate pattern in arr-2-GFP and arr-3-GFP expressing cells (Figure 3, panels C and D). In contrast, there was no significant internalization of HA-A_{2B}-ARs in AS 108 cells lacking heterologously expressed arr-2-GFP or arr-3-GFP (data not shown). Following agonist removal and a 30-min washout in the presence of the antagonist XAC (10 μM), nearly all the HA-A_{2B}AR had recycled back to the cell surface in arr-3-GFP expressing cells (Figure 3, panel F). Conversely, receptor recycling in arr-2-GFP cells was significantly slower, with a large percentage of the receptors remaining intracellular even after a 30-min washout (Figure 3, panel E). HA-A_{2B}AR recycling in arr-2-GFP cells was ultimately observed at later time points (60 min) with the majority of receptors returning to the cell surface. Thus, the agonist-dependent temporal and spatial redistribution of HA-A_{2B}AR observed by immunofluorescence microscopy is consistent with our analysis of receptor internalization/recycling measured by ELISA (Figure 2).

To further characterize the intracellular localization of A_{2B}-ARs, we used rab-5, a small G protein that is a marker for

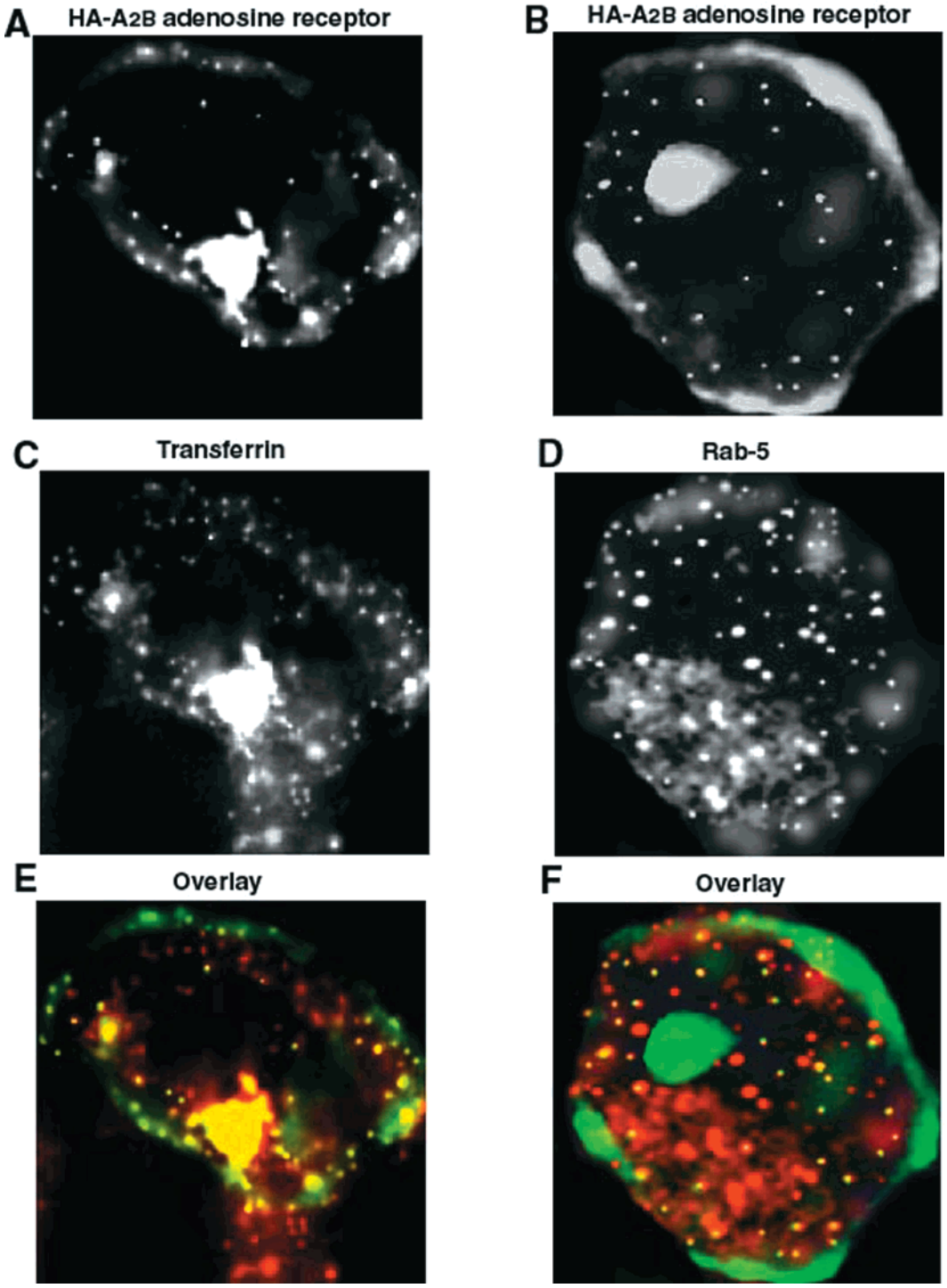

FIGURE 4: Colocalization of internalized HA-A_{2B}AR with transferrin and rab-5 in HEK293 cells. HEK293 cells were transfected with 5 μg of HA-A_{2B}AR and then split onto poly-L-lysine-coated glass coverslips. HA-A_{2B}AR was visualized with a fluorescein-conjugated HA antibody (A and B) while transferrin was localized using rhodamine-labeled transferrin (C). Prior to stimulation and viewing, coverslips were mounted in a chamber as described in Experimental Procedures. NECA (100 μM) was added and the redistribution of HA-A_{2B}AR and transferrin was monitored in real time as described in Experimental Procedures. Rab-5 localization (D) was determined in fixed cells following NECA addition using a rab-5 specific primary antibody and a rhodamine-labeled secondary antibody as described in Experimental Procedures. Images shown were obtained 45 min after agonist addition. The high degree of receptor/transferrin (E) and receptor/rab-5 (F) colocalization following agonist addition can be seen in the panels that overlay the A_{2B}AR (in green) and transferrin or rab-5 (in red) images (colocalization in yellow). Note that there is significant colocalization of receptor with transferrin (but not with rab-5) in an apparent endocytic recycling compartment.

early endosomes (*24*), and transferrin which binds to transferrin receptors and labels early endosomes and the endocytic recycling compartment (*25*). Following agonist-induced internalization (NECA; 30 min), the HA-A_{2B}AR displayed significant colocalization with transferrin in both small puncta and in a large perinuclear compartment (Figure 4, panel E). In contrast, the internalized HA-A_{2B}AR colocalized with rab-5 only in small puncta (Figure 4, panel F).

Numerous studies have shown that activation of several different GPCRs leads to a rapid recruitment of arr-2-GFP

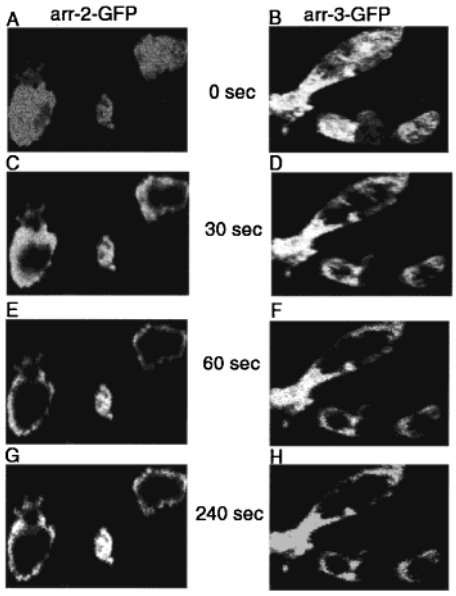

FIGURE 5: Agonist-induced redistribution of arr-2-GFP and arr-3-GFP. HEK293 cells were transfected with 5 μg of HA-A_{2B}AR and 0.25 μg arr-2-GFP or arr-3-GFP and then split onto poly-L-lysine-coated glass coverslips. HA-A_{2B}AR was visualized using a rhodamine-conjugated HA antibody. Prior to stimulation and viewing, coverslips were mounted in a chamber at 37 °C as described in Experimental Procedures. The initial diffuse cytoplasmic distribution of arr-2-GFP and arr-3-GFP is shown in panels A and B, respectively. NECA (100 μM) was added, and redistribution of arrestins was monitored in real time as described in Experimental Procedures. Images shown were obtained 30 (C and D), 60 (E and F), and 240 s (G and H) after agonist addition.

and arr-3-GFP from cytosol to membrane (*26*−*28*). Thus, to further explore the specificity of arrestins for the A_{2B}AR, we studied the effects of HA-A_{2B}AR activation on redistribution of arr-2-GFP and arr-3-GFP. HEK293 cells cotransfected with HA-A_{2B}AR and arr-2-GFP or arr3-GFP were stimulated with NECA (100 μM). Prior to agonist stimulation, both arrestins displayed a diffuse cytoplasmic distribution (Figure 5, panels A and B). Following agonist addition, a rapid translocation of arr-2-GFP (Figure 5, panels C, E, and G) and arr-3-GFP (Figure 5, panels D, F, and H) from cytosol to membrane was observed. No translocation was evident in cells that expressed arr-2-GFP or arr-3-GFP in the absence of HA-A_{2B}AR expression (data not shown).

Previous studies from this and other laboratories have revealed that more prolonged receptor activation (>10 min) can lead to a receptor-specific redistribution of arrestin-2/3-GFP into a punctate pattern that colocalizes with GPCRs in an endosomal compartment (*27*, *29*−*31*). Prior to agonist stimulation, arr-2-GFP displayed a diffuse cytoplasmic distribution (Figure 6, panel C), whereas the HA-A_{2B}ARs were primarily localized at the cell surface (Figure 6, panel A). Following a 20-min stimulation with NECA, the HA-A_{2B}ARs visibly redistributed into a distinct punctate pattern (Figure 6, panel B). Interestingly, arr-2-GFP also partially redistributed into a distinct punctate pattern (Figure 6, panel D) that exhibited a significant degree of colocalization with the HA-A_{2B}AR (Figure 6, panel F). In contrast, there was no redistribution of arr-3-GFP into a punctate pattern after membrane recruitment of this protein, despite a redistribution of HA-A_{2B}ARs similar to that observed in arr-2-GFP expressing cells (data not shown).

The colocalization of arr-2-GFP with HA-A_{2B}AR was further characterized in arrestin antisense cells (Figure 7). Following NECA stimulation, the HA-A_{2B}AR again internalized into a distinct punctate pattern that displayed a significant degree of colocalization with arr-2-GFP. Following agonist removal and a 30-min washout in the presence of XAC, a significant amount of HA-A_{2B}ARs remained inside the cell, predominantly in what is most likely an endocytic recycling compartment (colocalizes with transferrin but not rab-5) (Figure 4, panels E and F), with lesser amounts in early endosomes (colocalizes with rab-5 and transferrin) (Figure 4, panels E and F). Arr-2-GFP continued to associate with receptor in these rab5-containing early endosomes but was not seen in the endocytic recycling compartment. At later time points (60 min shown), arr-2-GFP had returned to a diffuse cytoplasmic distribution with the remaining internalized receptor still in a recycling compartment.

DISCUSSION

In a previous study, we found that the agonist-specific desensitization of A_{2B}ARs was significantly attenuated in cells with reduced arrestin levels (*22*). Thus, endogenous arrestins appear to play an important role in regulating the rapid agonist-promoted desensitization of the A_{2B}ARs in HEK293 cells. Since arrestins have been reported to mediate trafficking of a number of GPCRs (*10*−*12*), we investigated the role of arrestins in A_{2B}AR endocytosis and recycling in HEK293 cells.

Initial studies focusing on agonist-induced internalization of overexpressed HA-A_{2B}ARs revealed that reductions in endogenous arrestin expression effectively reduced receptor internalization. To confirm that reduced arrestin expression rather than nonspecific effects were responsible for the decreased receptor internalization, receptors were transiently coexpressed with arrestin-2 or arrestin-3. It was also hoped that these studies would uncover any possible differences in arrestin specificity. Overexpression of arrestin-2 or arrestin-3 (~10-fold over basal) in AS 108 cells (which display the greatest reduction in endogenous arrestin levels) was sufficient to restore receptor internalization to that of control cells. These results suggest that arrestin-2 and arrestin-3 are comparable in their effectiveness in A_{2B}ARs internalization.

Because our earlier experiments had shown resensitization of endogenous A_{2B}ARs was greatly impaired in arrestin antisense-expressing cells, experiments were undertaken to characterize the recycling of the A_{2B}AR receptor following agonist-induced internalization. Consistent with our studies on endogenous A_{2B}ARs receptors, HA-A_{2B}AR recycling was greatly impaired in cells with reduced arrestin levels. Again overexpression of either arrestin-2 or arrestin-3 in AS 108 cells rescued A_{2B}AR recycling. Interestingly, arrestin-3 proved more effective than arrestin-2 in increasing the rate of the recycling process. These findings were confirmed in immunofluorescence studies that also showed a reduced rate of HA-A_{2B}AR recycling in AS 108 cells expressing arr-2-GFP versus cells expressing arr-3-GFP. This is the first study to demonstrate that the two nonvisual arrestin isoforms can differentially affect receptor recycling after arrestin-dependent internalization.

To further investigate arrestin-2/3 specificity, we examined the agonist-induced movement of arr-2-GFP or arr-3-GFP.

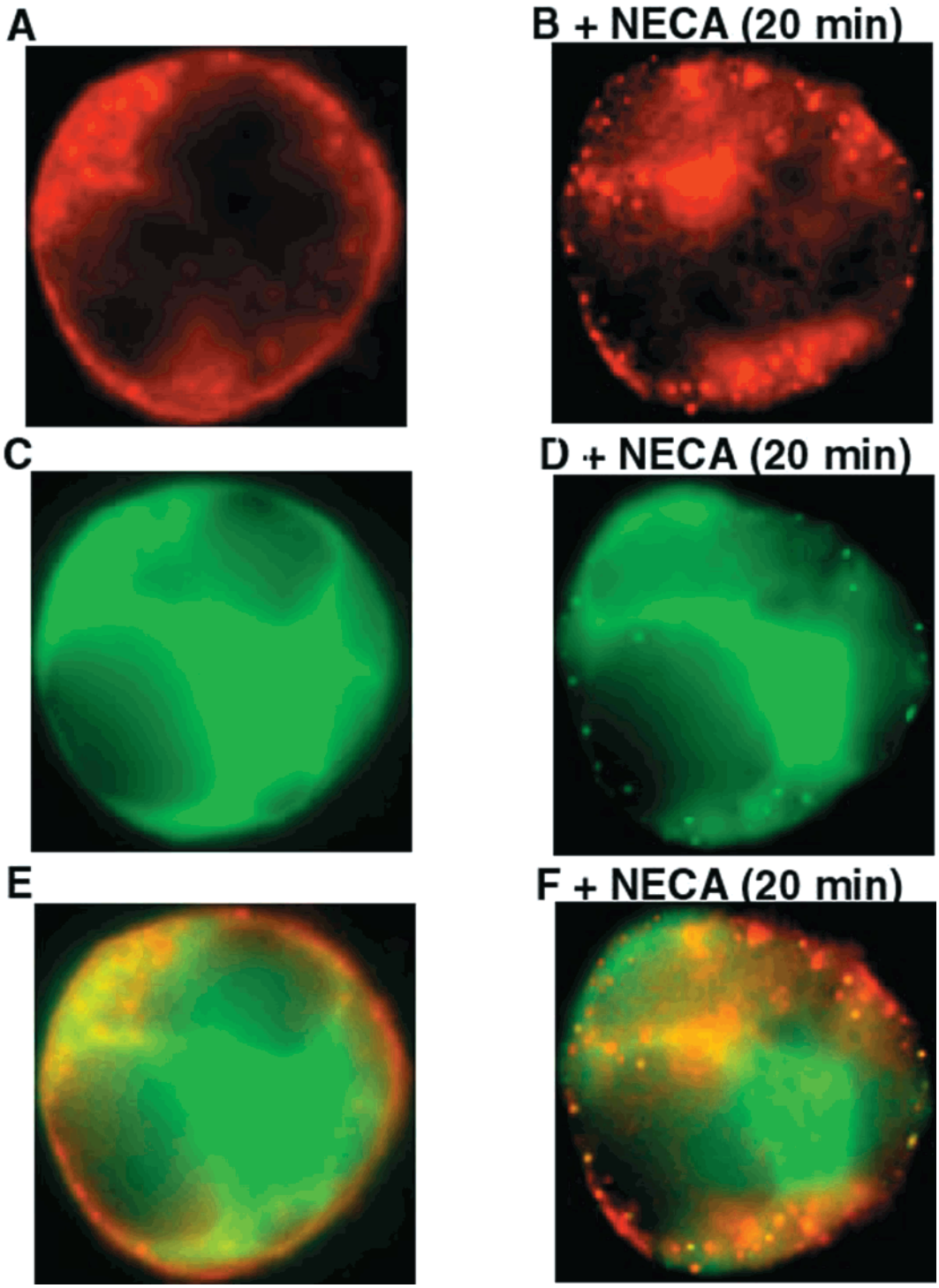

FIGURE 6: Agonist-induced redistribution of HA-A_{2B}AR and arr-2-GFP into early endosomes. HEK293 cells were transfected with 5 μg of HA-A_{2B}AR and 0.25 μg of arrestin-2-GFP and then split onto poly-L-lysine-coated glass coverslips. HA-A_{2B}AR was visualized with a rhodamine-conjugated HA antibody (A and B, in red). Prior to stimulation and viewing, coverslips were mounted in a chamber at 37 °C as described in Experimental Procedures. The initial membrane localization of receptor and diffuse cytoplasmic distribution of arr-2-GFP is shown in panels A and C, respectively. NECA (100 μM) was added, and redistribution of arrestins was monitored in real time as described in Experimental Procedures. Images shown were obtained 20 min (B and D) after agonist addition. The significant amount of arrestin and receptor colocalization following agonist addition can be seen in panel F, which is formed by overlay of the arr-2-GFP (in green) and HA-A_{2B}AR (in red) images.

Several studies have utilized this approach to provide real-time analysis of receptor−arrestin interactions in single cells overexpressing various GPCRs (*26*−*28*). Both arr-2-GFP and arr-3-GFP underwent rapid agonist-dependent translocation from the cytosol to the plasma membrane in cells coexpressing HA-A_{2B}ARs. Within this time frame, there was no apparent movement of arrestin in HEK293 cells that did not coexpress HA-tagged receptor, even though these cells endogenously express A_{2B}ARs (*32*). We have consistently failed to observe rapid translocation of arrestins from the cytosol to the membrane upon activation of any endogenous GPCRs that we have examined thus far (*31*). We attribute this to low levels of endogenous GPCR expression, which may limit the ability to recruit a sufficient amount of arrestin

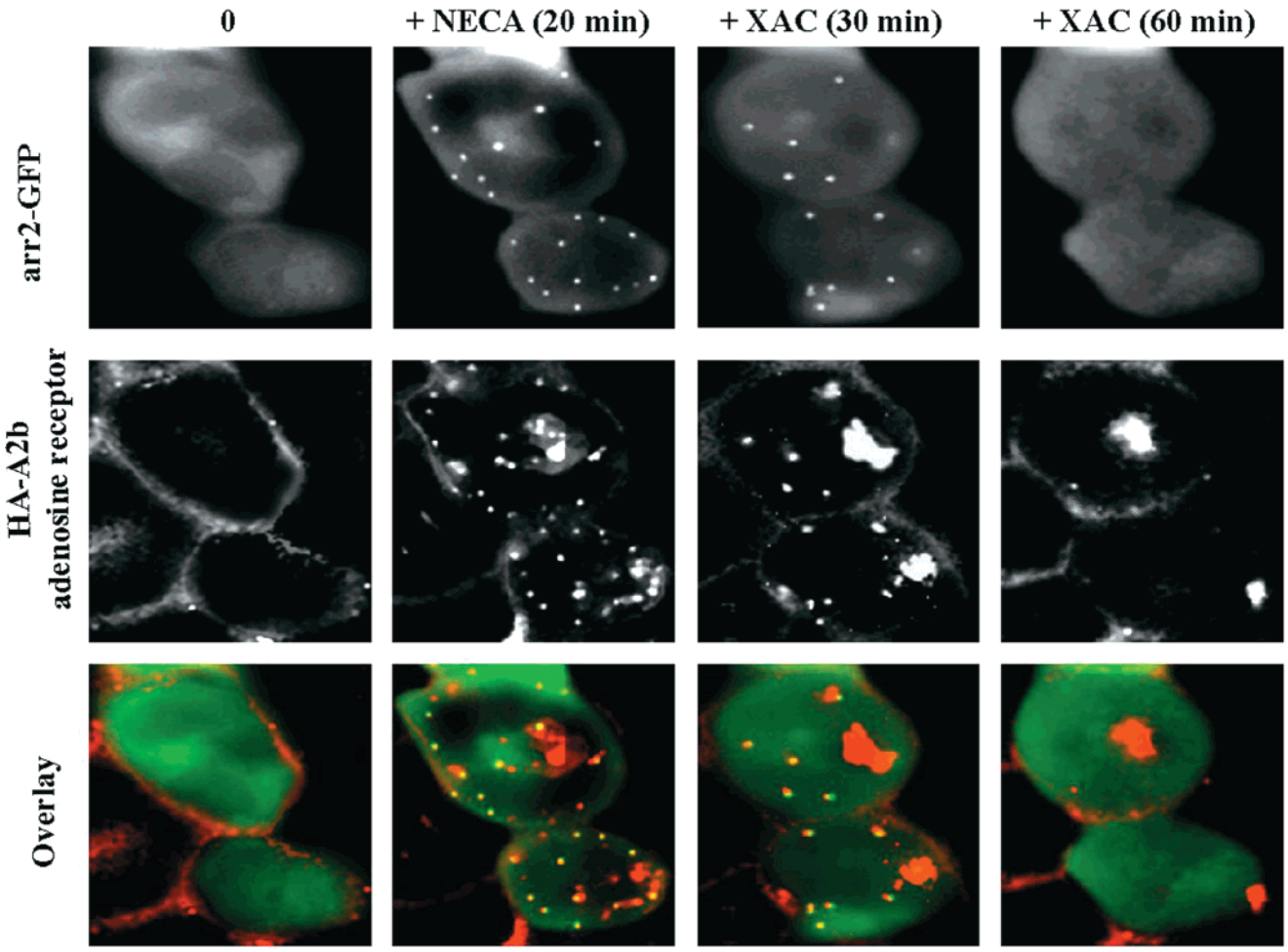

FIGURE 7: Agonist-induced redistribution and subsequent recycling of HA-A_{2B}AR and arr-2-GFP. AS 108 cells were transfected with 5 μg of HA-A_{2B} adenosine receptor and 0.25 μg of arr-2-GFP and then split onto poly-L-lysine-coated glass coverslips. HA-A_{2B} adenosine receptor was visualized with a rhodamine-conjugated HA antibody. Prior to stimulation and viewing, coverslips were mounted in a chamber at 37 °C as described in Experimental Procedures. The initial membrane localization of receptor and diffuse cytoplasmic distribution of arr-2-GFP is shown at time 0. NECA (100 μM) was added, and the redistribution of arrestin and receptor was monitored in real time as described in Experimental Procedures. Cells were then washed five times with warmed DMEM containing the adenosine receptor antagonist XAC (100 μM), and the redistribution of receptor again was monitored in real time. Images shown were 30 and 60 min after agonist washout/antagonist addition. The high degree of arrestin and receptor colocalization following agonist addition can be seen in the overlay of the arr-2-GFP (in green) and HA-A_{2B}AR (in red) images. Note that there is little or no colocalization of arr-2-GFP with receptor in the larger putative endocytic recycling compartment.

that is visible by conventional immunofluorescence microscopy.

Following more prolonged agonist treatments (>10 min), arr-2-GFP colocalized with HA-tagged A_{2B}ARs in an early endosomal population as indicated by colocalization with rab-5. In contrast, arr-3-GFP alternatively appeared to dissociate from the A_{2B}AR at the plasma membrane after A_{2B}AR endocytosis. This is the first demonstration that arrestin-2 and arrestin-3 redistribute differently. It will be interesting in future studies to investigate the structural differences between these two isoforms that confer the specificity of this redistribution.

A number of previous studies have shown that nonvisual arrestins can traffic with internalized GPCRs into early endosomes (*27*, *29*−*31*). In agreement with these studies, we find that both HA-A_{2B}ARs and arr-2-GFP colocalize with transferrin and rab-5 in an early endosomal population. A_{2B}-ARs also accumulated in a distinct structure near the nucleus following agonist stimulation. The perinuclear localization of the receptor, which colocalized with transferrin receptor but not rab-5 (Figure 3), is indicitive of the pericentriolar recycling compartment that serves as a compartment for controlling and recycling of membrane proteins (*33*). At steady state, transferrin accumulates in this recycling compartment, since the rate-limiting step in recycling is transport from this location (*34*). Membrane proteins destined for recycling are rapidly transported from the early, sorting endosome to the pericentriolar recycling compartment and are subsequently directed back to the plasma membrane (*35*). However, arr-2-GFP does not colocalize with HA-A_{2B}AR once the receptor enters this putative endosomal recycling compartment. Therefore, we conclude that arrestin-2 dissociates from the receptor prior to it entering the endocytic recycling compartment.

The function of prolonged arrestin-2/A_{2B}AR association (as compared to that of arrestin-3/A_{2B}AR) in an endosomal compartment is unknown. In AS 108 cells, A_{2B}AR recycling is slower in cells overexpressing arrestin-2 versus arrestin-3. Therefore, it is intriguing to speculate that association of arrestin-2 with A_{2B}AR in endosomes delays subsequent receptor dephosphorylation, recycling, and resensitization. Although it is unclear why arrestin-2 displays this continued

association with the A_{2B}AR, there are a number of plausible explanations, including potential higher affinity binding between A_{2B}AR and arrestin-2. Our findings are similar to a recent study that demonstrated that the prolonged association of arrestin-3 with the V2 vasopressin receptor correlates with a delay in receptor resensitization (*30*). In that study, the ability of arrestin-3 to remain associated with desensitized GPCRs in endosomes was mediated by a specific cluster of phosphorylated serine residues in the vasopressin receptor carboxyl-terminal tail. The A_{2B}AR lacks such a sequence motif indicating that different determinants are likely responsible.

Few functional differences between arrestin-2 and arrestin-3 have been reported. This study is the first to show that although arrestin-2 and arrestin-3 appear comparable in their ability to mediate agonist-induced receptor internalization, isoform binding subsequently dictates the differential kinetics of A_{2B}AR recycling and resensitization. Future studies will explore this phenomena with additional receptor subtypes and investigate the structural determinants of GPCRs and arrestins that contribute to differential arrestin/receptor association.

ACKNOWLEDGMENT

We thank R. Penn for critical reading of the manuscript and members of the Benovic lab for helpful discussions.

REFERENCES

1. Olah, M. E., and Stiles, G. L. (1995) *Annu. Rev. Pharmacol. Toxicol. 35*, 581−606.
2. Feoktistov, I., and Biaggioni, I. (1997) *Pharmacol. Rev. 49*, 381−402.
3. Linden J., Thai T., Figler H., Jin X., and Robeva A. S. (1999) *Mol. Pharmacol. 56*, 705−713.
4. Mundell, S. J., and Kelly, E. (1998) *Biochem. Pharmacol. 55*, 595−603.
5. Mundell, S. J., Benovic, J. L., and Kelly, E. (1997) *Mol. Pharmacol. 51*, 991−998.
6. Mundell, S. J., Luty, J. S., Willets, J., Benovic, J. L., and Kelly, E. (1998) *Br. J. Pharmacol. 125*, 347−356.
7. Carman, C., and Benovic, J. L. (1998) *Curr. Opin. Neurobiol. 8*, 335−344.
8. Kuhn, H., Hall, S. W., and Wilden, U. (1984) *FEBS Lett. 176*, 473−478.
9. Krupnick, J. G., Gurevich, V. V., and Benovic, J. L. (1997) *J. Biol. Chem. 272*, 18125−18131.
10. Ferguson, S. S. G., Downey, W. E. I., Colapietro, A.-M., Barak, L. S., Menard, L., and Caron, M. G. (1996) *Science 271*, 363−365.
11. Goodman, O. B., Jr., Krupnick, J. G., Santini, F., Gurevich, V. V., Penn, R. B., Gagnon, A. W., Keen, J. H., and Benovic, J. L. (1996) *Nature 383*, 447−450.
12. Krupnick, J. G., Benovic J. L. (1998) *Annu. Rev. Pharmacol. Toxicol. 38*, 289−319.
13. Zhang, J., Barak, L. S., Winkler, K. E., Caron, M. G., and Ferguson, S. S. G. (1997) *J. Biol. Chem. 272*, 27005−27014.
14. Ferguson, S. S. G., Barak, L. S., Zhang, J., and Caron, M. G. (1996) *Can. J. Physiol. Pharmacol. 74*, 1095−1110.
15. Krupnick, J. G., Goodman, O. B., Jr., Keen, J. H., and Benovic, J. L. (1997) *J. Biol. Chem. 272*, 15011−15016.
16. Laporte, S. A., Oakley, R. H., Zhang, J., Holt, J. A., Ferguson, S. S., Caron, M. G., and Barak, L. S. (1999) *Proc. Natl. Acad. Sci. U.S.A. 96*, 3712−3717.
17. Yu, S. S., and Lefkowitz, R. J. (1993) *J. Biol. Chem. 268*, 337−341.
18. Pippig, S., Andexinger, S., and Lohse, M. J. (1995) *Mol. Pharmacol. 47*, 666−676.
19. Krueger, K. M., Daaka, Y., Pitcher J. A., and Lefkowitz, R. J. (1997) *J. Biol. Chem. 272*, 5−8.
20. Bogatkewitsch, G. S., Lenz, W., Jakobs K. H., and Van Koppen, C. J. (1996) *Mol. Pharmacol. 50*, 424−429.
21. Mundell, S. J., and Kelly, E. (1998) *Br. J. Pharmacol. 125*, 1594−1600.
22. Mundell, S. J., Loudon, R. P., and Benovic J. L. (1999) *Biochemistry 38*, 8723−8732.
23. Daunt, D. A., Hurt, C., Hein L., Kallio, J., Feng, F., and Kobilka, B. K. (1997) *Mol. Pharmacol. 51*, 711−720.
24. Mohrmann, K., and van der Sluijs, P. (1999) *Mol. Membr. Biol. 16*, 81−87.
25. Cao, T. T., Mays, R. W., and von Zastrow, M. (1998) *J. Biol. Chem. 273*, 24592−24602.
26. Barak, L. S., Ferguson, S. S., Zhang, J., and Caron, M. G. (1997) *J. Biol. Chem. 272*, 27497−27500.
27. Groarke, D. A., Wilson, S., Krasel, C., and Milligan, G. (1999)- *J. Biol. Chem. 274*, 23263−23269.
28. Barak, L. S., Warabi, K., Feng, X., Caron, M. G., and Kwatra, M. M. (1999) *J. Biol. Chem. 274*, 7565−7569.
29. McConalogue, K., Dery, O., Lovett, M., Wong, H., Walsh, J. H., Grady, E. F., and Bunnett, N. W. (1999) *J. Biol. Chem. 274*, 16257−16268.
30. Oakley, R. H., Laporte, S. A., Holt, J. A., Barak, L. S., and Caron, M. G. (1999) *J. Biol. Chem. 274*, 32248−32257.
31. Mundell, S. J. and Benovic, J. L. (2000) *J. Biol. Chem. 275*, 12900−12908.
32. Cooper, J., Hill S. J., and Alexander, S. P. H. (1997) *Br. J. Pharmacol. 122*, 546−550.
33. Mayor, S., Presley, J. F., and Maxfield, F. R., (1993) *J. Cell. Biol. 121*, 1257−1269.
34. Presley, J. F., Mayor, S., Dunn K. W., Johnson, L. S., McGraw, T. E., and Maxfield, F. R. (1993) *J. Cell. Biol. 122*, 1231−1241.
35. Ghosh, R. N. and Maxfield, F. R. (1995) *J. Cell. Biol. 128*, 549−561.

BI0010928